

## Interfacial Engineering of Silicon Carbide Nanowire/Cellulose Microcrystal Paper towards High Thermal Conductivity

Yimin Yao,<sup>†,‡</sup> Xiaoliang Zeng,<sup>\*,†,‡</sup> Guiran Pan,<sup>†,§</sup> Jiajia Sun,<sup>†,||</sup> Jiantao Hu,<sup>†,||</sup> Yun Huang,<sup>†,||</sup> Rong Sun,<sup>\*,†</sup> Jian-Bin Xu,<sup>⊥</sup> Ching-Ping Wong<sup>†,⊥,#</sup>

<sup>†</sup>Shenzhen Institutes of Advanced Technology, Chinese Academy of Sciences, Shenzhen 518055, China.

<sup>‡</sup>Shenzhen College of Advanced Technology, University of Chinese Academy of Sciences, Shenzhen 518055, China.

<sup>§</sup>Department of Chemical Engineering, China University of Petroleum, Beijing 102249, China.

<sup>||</sup>Department of Nano Science and Technology Institute, University of Science and Technology of China, Suzhou 215123, China.

<sup>⊥</sup>Department of Electronics Engineering, The Chinese University of Hong Kong, Hong Kong 999077, China.

<sup>#</sup>School of Materials Science and Engineering, Georgia Institute of Technology, Atlanta, Georgia 30332, United States.

\*Address corresponding to xl.zeng@siat.ac.cn and rong.sun@siat.ac.cn. Tel. 86-755-86392158. Postal address: 1068 Xueyuan Avenue, Shenzhen University Town, Shenzhen, China.

### Contents:

- Figure S1. Length distribution of SiCNWs.
- Figure S2. Length distribution of CMCs.
- Figure S3. Dispersity of SiCNW and SiCNW–Ag. (a) Optical images of initially prepared SiCNWs and SiCNW–Ag dispersions. Optical image of (b) SiCNW and (c) SiCNW–Ag after standing for 48 h. The red circle indicates the existence of SiCNW agglomeration.
- Figure S4. TEM images of SiCNW–Ag generated by different volume ratios of SiCNW to Ag.
- Figure S5. Characterization and thermal conductivity of SiCNW/CMC paper containing free AgNPs. (a) Optical images of SiCNWs, CMC, Ag dispersion, and their mixture. Optical image (b) and surface morphology (c) of composite paper containing free AgNPs. (d) Comparison of in-plane thermal conductivities of the composite papers with three kinds of filler.
- Figure S6. The cross-section morphology of SiCNW–Ag/CMC composite paper with a filler content of 90 vol%.
- Figure S7. Out-plane thermal conductivities of SiCNW/CMC and SiCNW–Ag/CMC composite papers with filler loadings of 50 vol% and 90 vol%.
- Figure S8. A representative SEM image for  $\theta$  calculation.

- Figure S9. Cross-section microstructures of (a) SiCNW/CMC and (b) SiCNW–Ag/CMC composite papers with 30 vol% filler content.
- Figure S10. Simulated thermal conductivities obtained by varying the  $\theta$  value in the EMT equation.
- Figure S11. Schematic used to derive the overlap area and length for two SiCNWs.
- Table S1. Parameters obtained from Foygel’s model for SiCNW/CMC and SiCNW-Ag/CMC composites.
- Theoretical approach used in the calculation of the average overlap area between two SiCNWs.

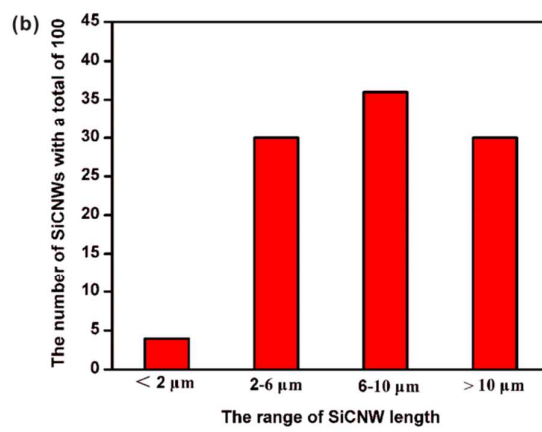
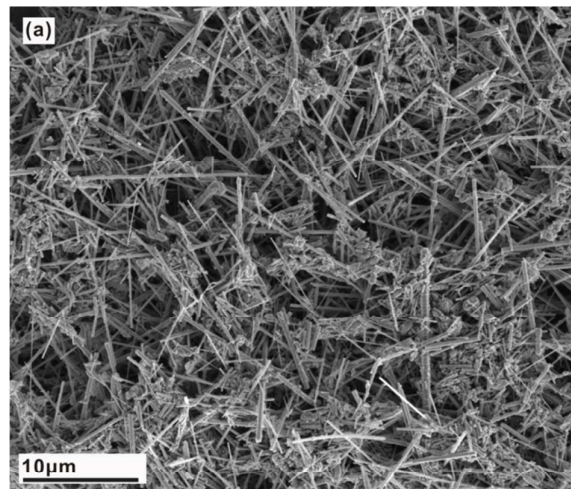


**Figure S1.** (a) SEM image and (b) Length distribution of SiCNWs.

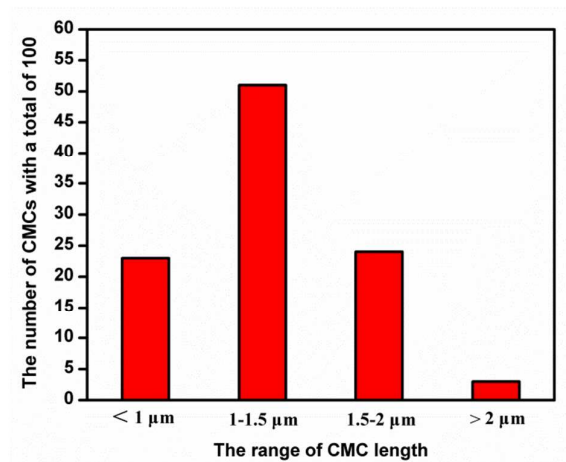


**Figure S2.** Length distribution of CMCs.

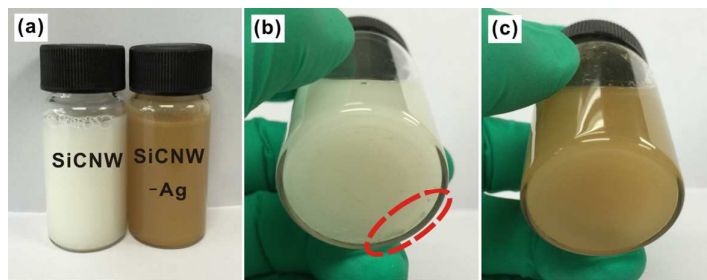


**Figure S3.** Dispersivity of SiCNW and SiCNW–Ag. (a) Optical images of initially prepared SiCNWs and SiCNW–Ag dispersions. Optical image of (b) SiCNW and (c) SiCNW–Ag after standing for 48 h. The red circle indicates the existence of SiCNW agglomeration.

The initially prepared SiCNWs and SiCNW–Ag possess good dispersivity in water (Figure S4a). However, a small amount of SiCNW agglomeration formed in SiCNW dispersion after standing for 48 h (red circle in Figure S4b). On the contrary, the dispersion of SiCNW–Ag still exhibits good stability (Figure S4c). Therefore, we viewed the abundant hydrophilic groups of PVP coated on AgNPs as the main reason for this phenomenon.

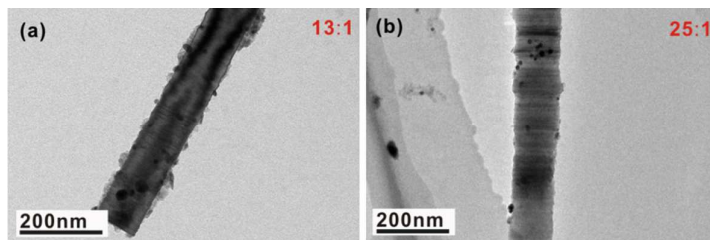


**Figure S4.** TEM images of SiCNW–Ag generated by different volume ratios of SiCNW to Ag.

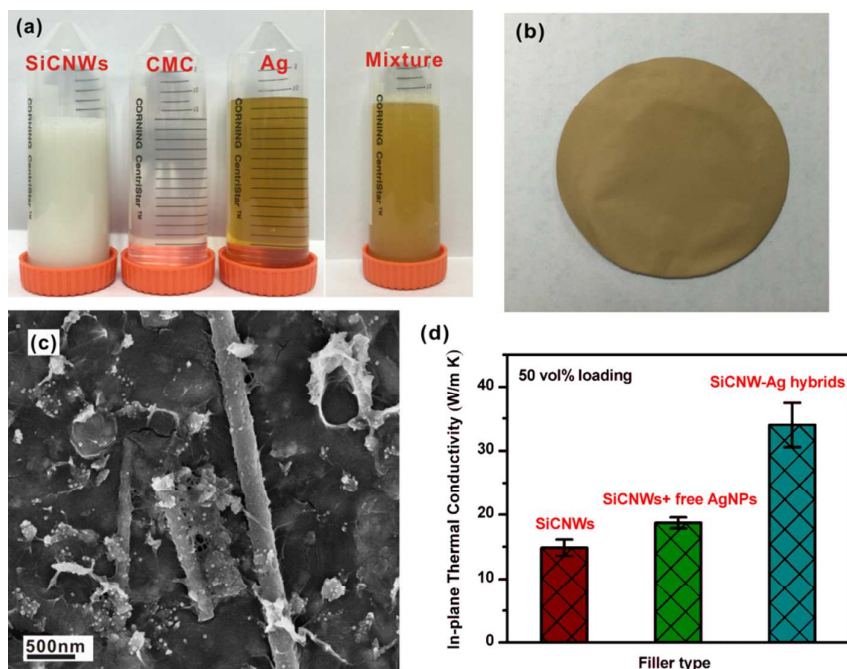


**Figure S5.** Characterization and thermal conductivity of SiCNW/CMC paper containing free AgNPs. (a) Optical images of SiCNWs, CMC, Ag dispersion, and their mixture. Optical image (b) and surface morphology (c) of composite paper containing free AgNPs. (d) Comparison of the in-plane thermal conductivity of the composite papers with three kinds of filler.

We have further fabricated composite paper containing CMC, SiCNWs, and free AgNPs (Figure S5a, b). The obtained surface morphology (Figure S5c) shows the existence of AgNPs both on SiCNWs and CMC. The corresponding thermal conductivity (Figure S5d) is much lower than that of the composite paper containing SiCNW–Ag hybrids, and a little higher than the one with pure SiCNWs. It indicates that although the addition of AgNPs is beneficial for thermal enhancement, being located on the surface of SiCNWs would greatly improve the enhancing efficiency of AgNPs.

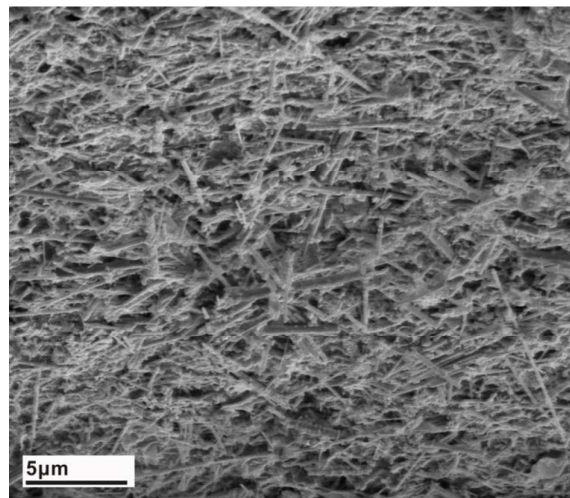


**Figure S6.** The cross-section morphology of SiCNW–Ag/CMC composite paper with a filler content of 90 vol%.

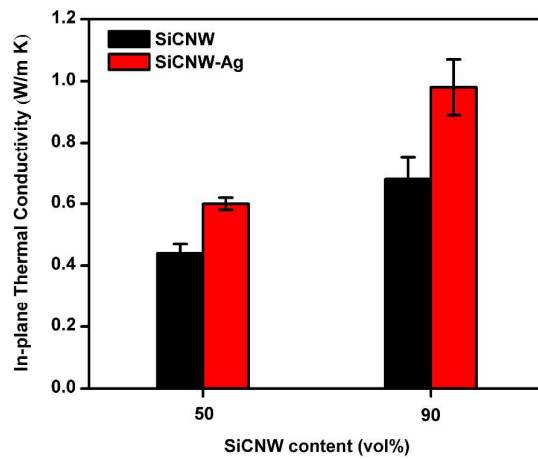


**Figure S7.** Out-plane thermal conductivities of SiCNW/CMC and SiCNW–Ag/CMC composite papers with filler loadings of 50 vol% and 90 vol%.

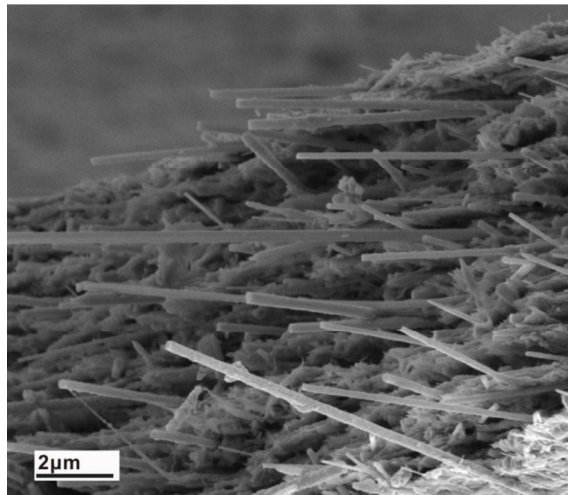


**Figure S8.** A representative SEM image for  $\theta$  calculation.

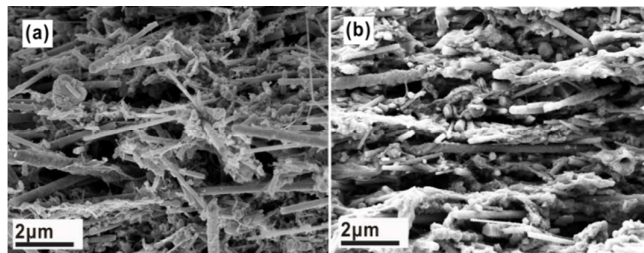


**Figure S9.** Microstructures of SiCNW/CMC and SiCNW–Ag/CMC composite papers. Cross-section microstructures of (a) SiCNW/CMC and (b) SiCNW–Ag/CMC composite papers with 30 vol% filler content.

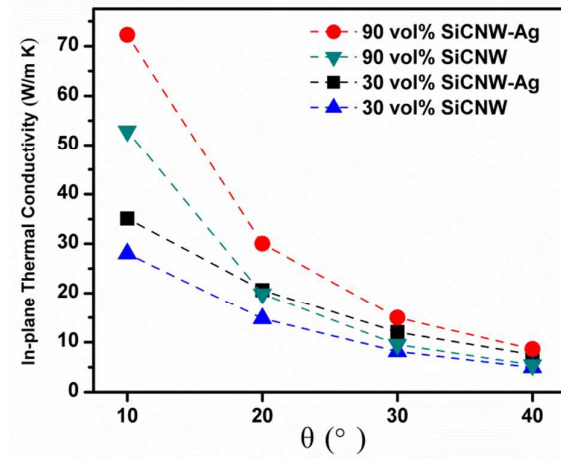
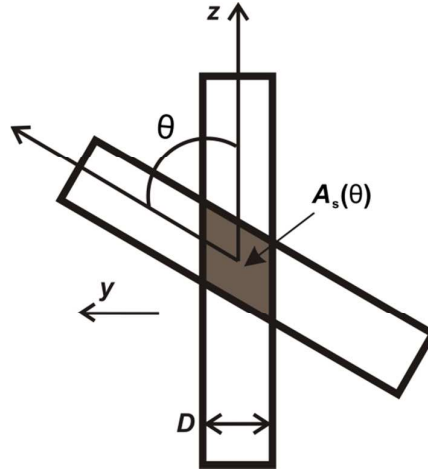


Figure S10. Simulated thermal conductivities obtained by varying the  $\theta$  value in the EMT equation.

**Table S1.** Parameters obtained from Foygel's model for SiCNW/CMC and SiCNW-Ag/CMC composites.

<b>Sample</b>	$K_0$	$V_c$	$t(p)$
<b>SiCNW/CNF</b>	148	0.08	1.6
<b>SiCNW-Ag/CNF</b>	250	0.08	1.6

**Theoretical approach used in the calculation of the average overlap area between two SiCNWs<sup>1</sup>**



**Figure S11.** Schematic used to derive the overlap area and length for two SiCNWs.

The average overlap area is calculated by applying a uniform orientation distribution and integrating over all orientations to obtain the formula

$$\overline{A_s} = \frac{2D^2}{\pi} \left[ \ln \left( \sin \left( \frac{\theta}{2} \right) \right) - \ln \left( \cos \left( \frac{\theta}{2} \right) \right) \right]_0^{\frac{\pi}{2}} \quad (\text{S1})$$

The above formulae suggest an infinite overlap area and distance for  $\theta=0$ , which is as expected for the infinite cylinder assumption used in developing the equations. For finite cylinders, the overlap area is the entire projected area of the cylinder, or  $DL$ . Therefore, a critical angle  $\theta_c$  may be defined such that

$$A_{s,c} = \frac{D^2}{\sin(\theta_c)} \quad (\text{S2})$$

Performing the intergration for  $\overline{A_s}$  results in the expression

$$\overline{A_s} = \frac{2D^2}{\pi} \delta(p) \quad (\text{S3})$$

where

$$\delta(p) = \ln \left[ \frac{\sqrt{1+p^{-1}} + \sqrt{1-p^{-1}}}{\sqrt{1+p^{-1}} - \sqrt{1-p^{-1}}} \right] \quad (\text{S4})$$

Here  $p$  is the aspect ratio of SiCNW. Using this equation we can obtain the average overlap area between two SiCNWs.

## REFERENCES

1. Wemhoff, A. P., Thermal Conductivity Predictions of Composites Containing Percolated Networks of Uniform Cylindrical Inclusions. *Int. J. Heat Mass Transfer* **2013**, *62*, 255-262.